Electronic Supplementary Material (ESI) for CrystEngComm.
This journal is © The Royal Society of Chemistry 2019

Effect of arrangement of functional groups on stability and gas adsorption properties in two regioisomeric copper bent diisophthalate frameworks

Tingting Xu, Zhenzhen Jiang, Minghui He, Xiaoxia Gao, and Yabing He*

Key Laboratory of the Ministry of Education for Advanced Catalysis Materials, College of Chemistry and Life Sciences, Zhejiang Normal University, Jinhua 321004, China. E-mail: heyabing@zjnu.cn

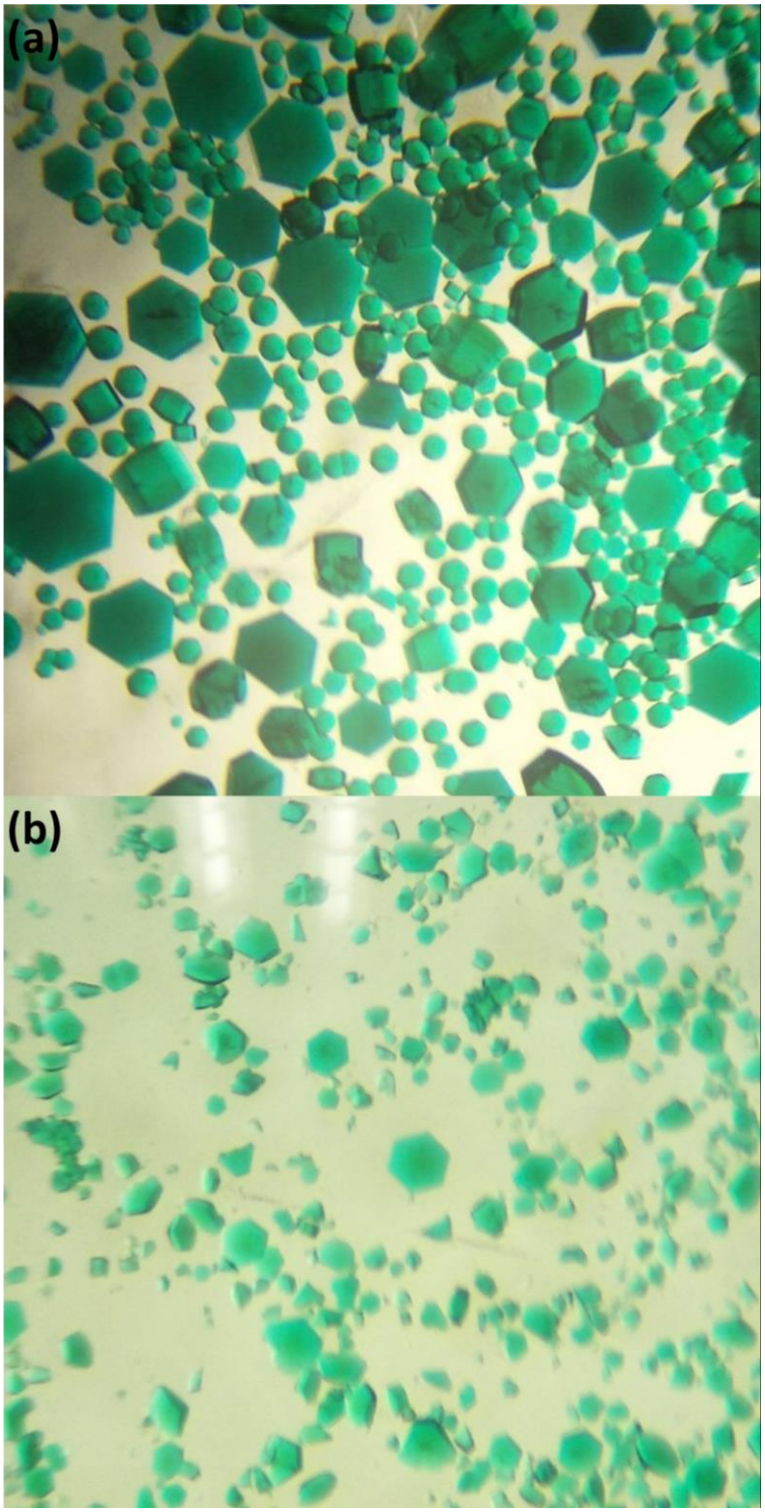

Fig. S0 Electronic photographs of the as-synthesized (a) **ZJNU-11** and (b) **ZJNU-12**.

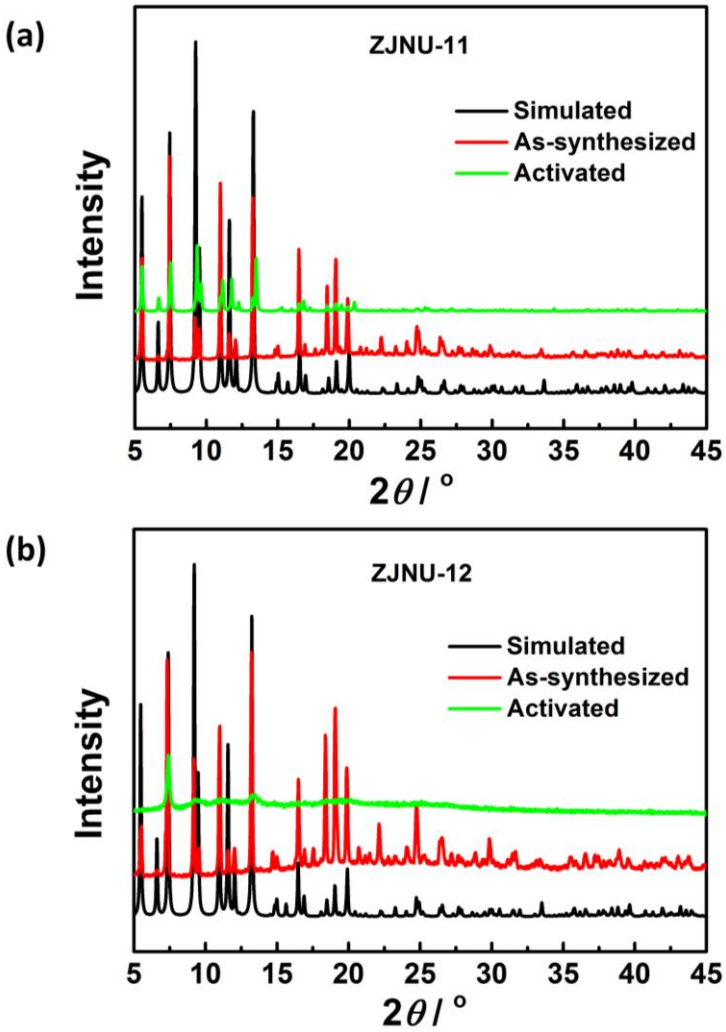

Fig. S1 Comparison of the experimental and simulated PXRD patterns of (a) **ZJNU-11** and (b) **ZJNU-12**.

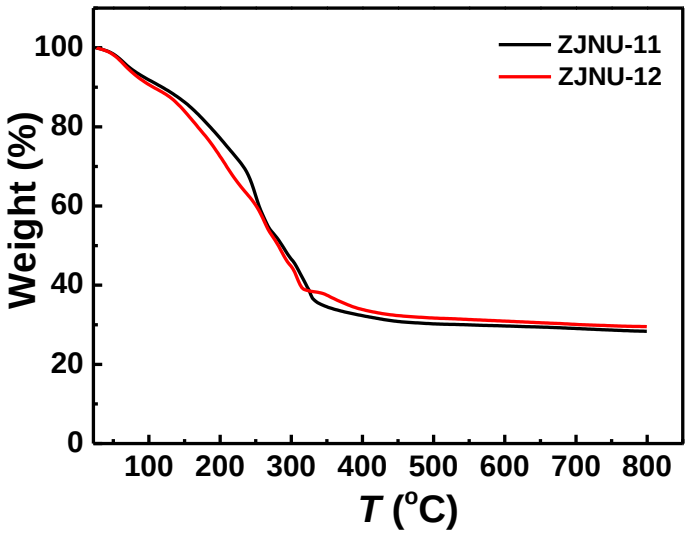

Fig. S2 TGA curves of the as-synthesized (a) **ZJNU-11** and (b) **ZJNU-12** under nitrogen atmosphere.

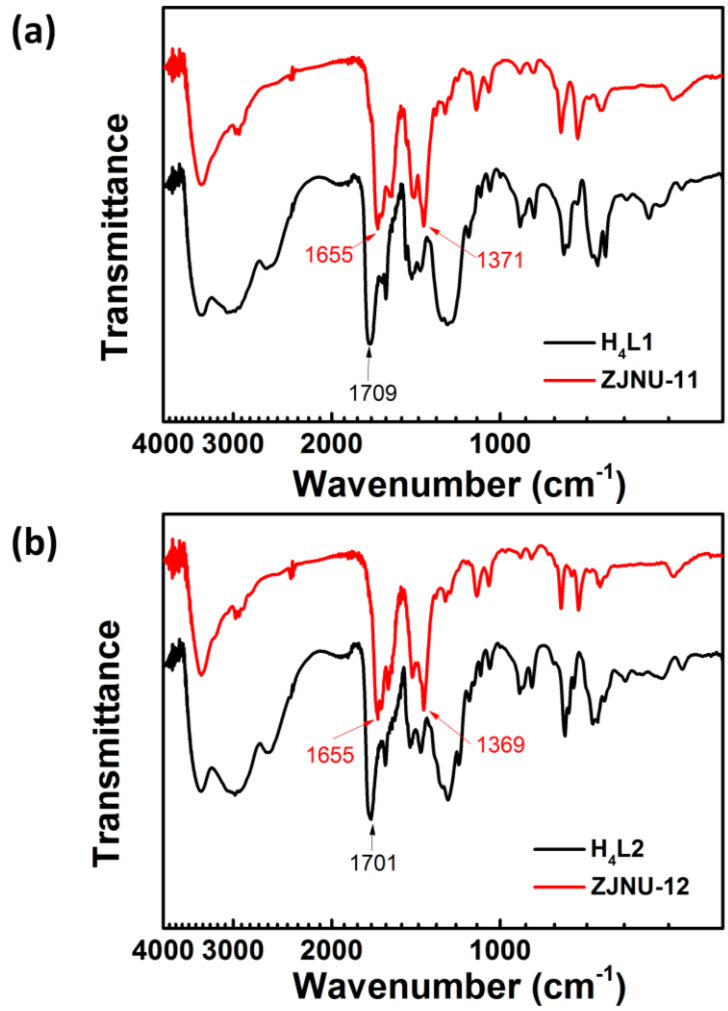

Fig. S3 Comparison of FTIR spectra of the diisophthalate ligands and their corresponding as-synthesized MOFs.

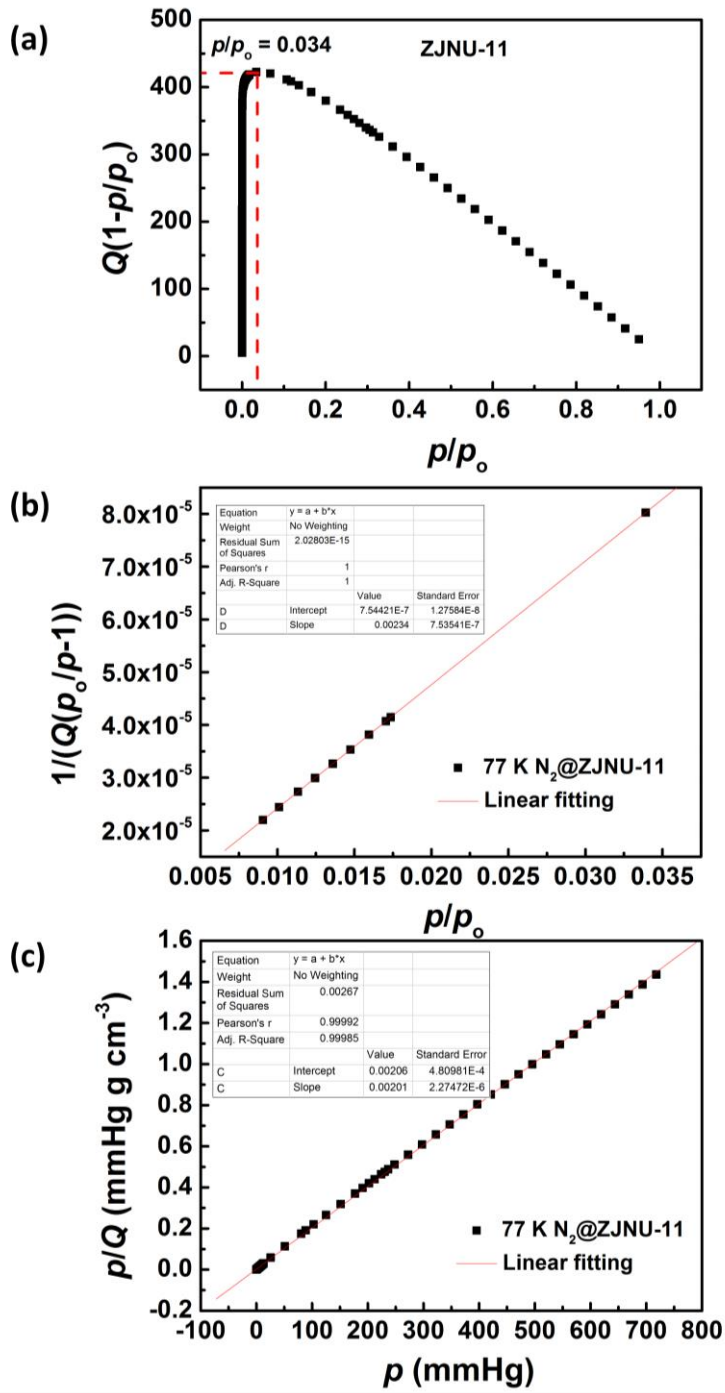

S_{BET} = 1/(7.54421 ×10^{-7}+ 0.00234)/22414 × 6.023 × 10^{23} × 0.162 × 10^{-18} = 1860 m^2 g^{-1}

$S_{Langmuir}$ = (1/0.00201)/22414 × 6.023 × 10^{23} × 0.162 × 10^{-18} = 2166 m^2 g^{-1}

BET constant C = 1 + 0.00234/7.54421 ×10^{-7} = 3103

$$(p/p_o)_{n_m} = \frac{1}{\sqrt{C}+1} = 0.01764$$

Fig. S4 The consistency plot (a), BET surface area plot (b), and Langmuir surface area plot (c) for **ZJNU-11**.

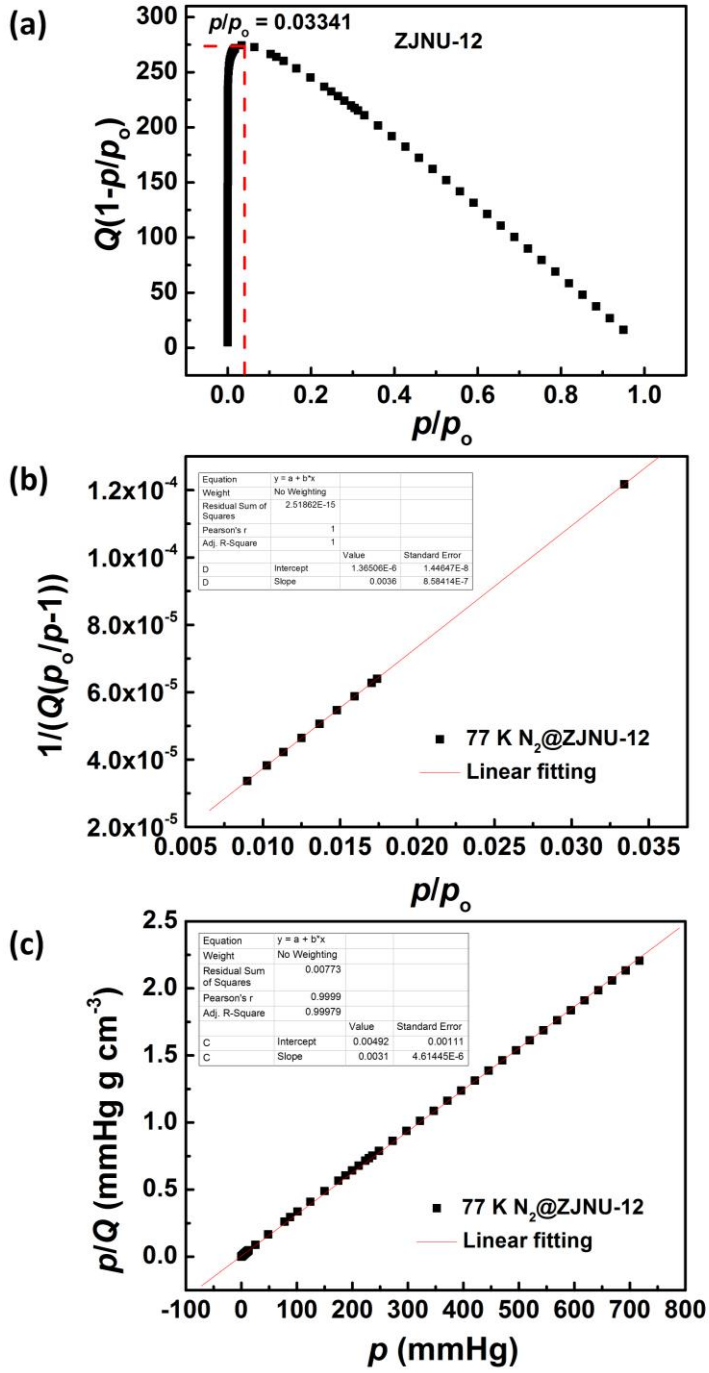

S_{BET} = 1/(1.36506×10^{-6}+ 0.0036)/22414 × 6.023 × 10^{23} × 0.162 × 10^{-18} = 1208 m^2 g^{-1}

$S_{Langmuir}$ = (1/0.0031)/22414 × 6.023 × 10^{23} × 0.162 × 10^{-18} = 1404 m^2 g^{-1}

BET constant C = 1 + 0.0036/1.36506×10^{-6} = 2638

$$(p/p_o)_{n_m} = \frac{1}{\sqrt{C}+1} = 0.0191$$

Fig. S5 The consistency plot (a), BET surface area plot (b), and Langmuir surface area plot (c) for **ZJNU-12**.

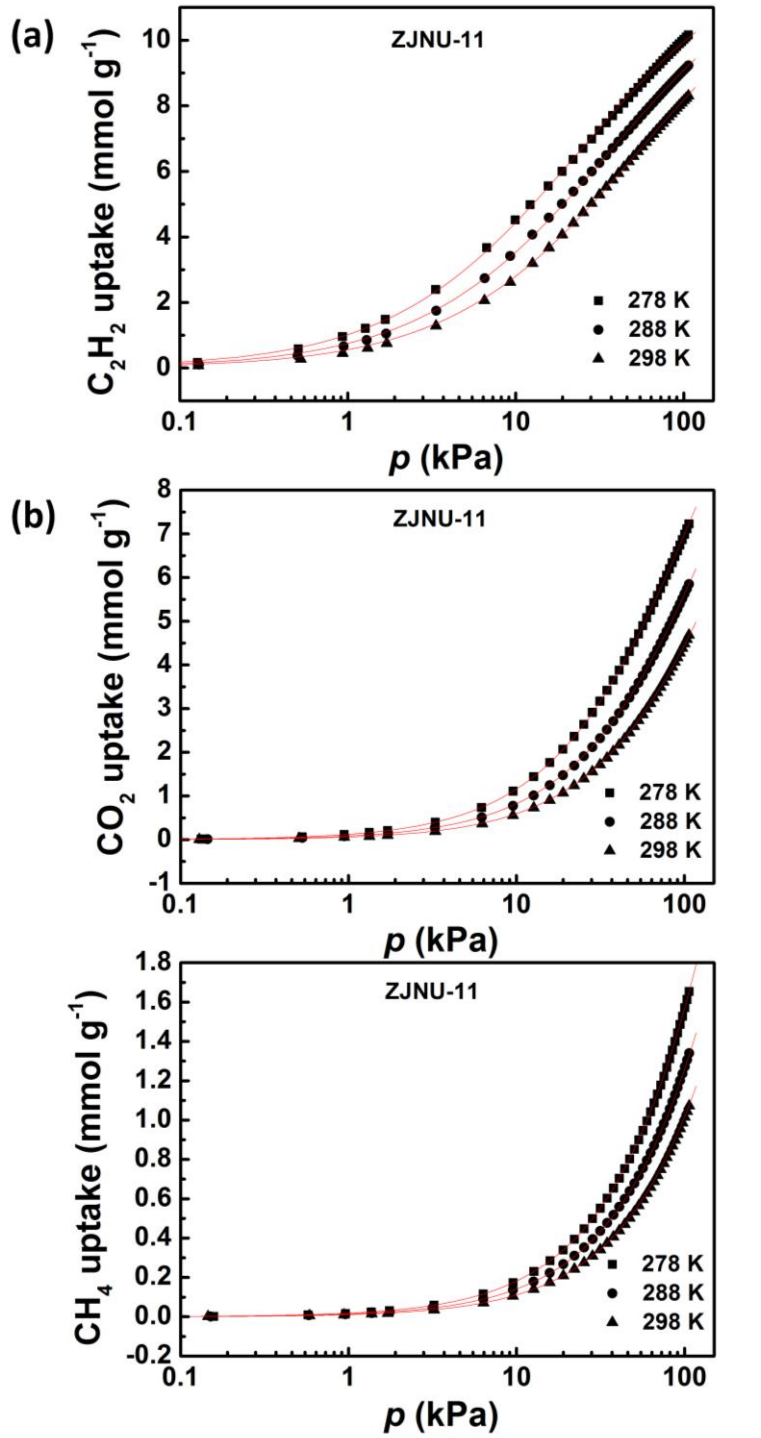

Fig. S6 Comparison of the pure-component isotherm data for (a) C_2H_2, (b) CO_2, and (c) CH_4 in **ZJNU-11** with the fitted isotherms at 278 K, 288 K, and 298 K.

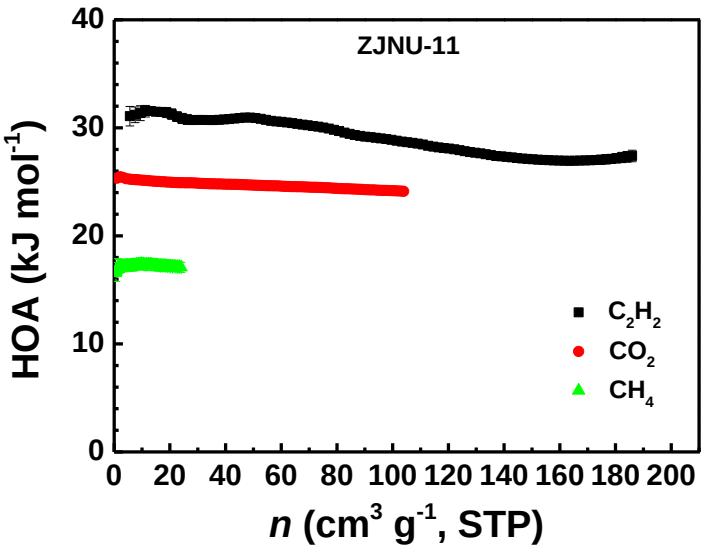

Fig. S7 The isosteric heat of C_2H_2, CO_2, and CH_4 adsorption in **ZJNU-11**.

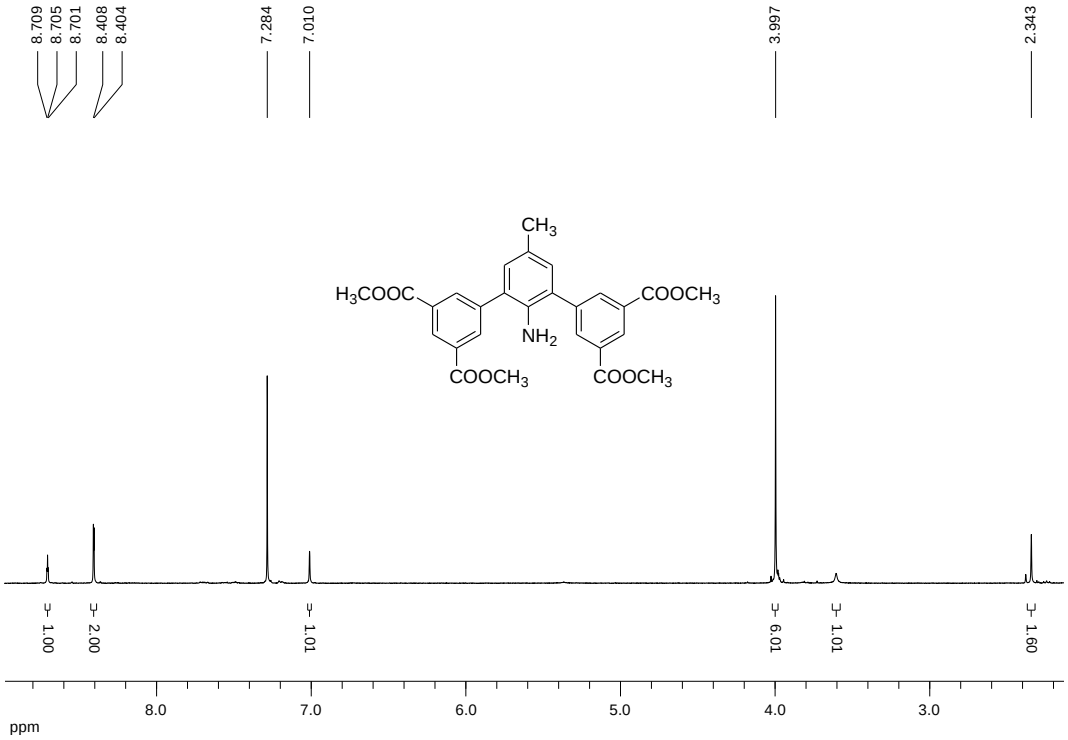
8.709
8.705
8.701
8.408
8.404
7.284
7.010
3.997
2.343
CH3
H3COOC
COOCH3
NH2
COOCH3
COOCH3
1.00
2.00
1.01
6.01
1.01
1.60
8.0
7.0
6.0
5.0
4.0
3.0
ppm

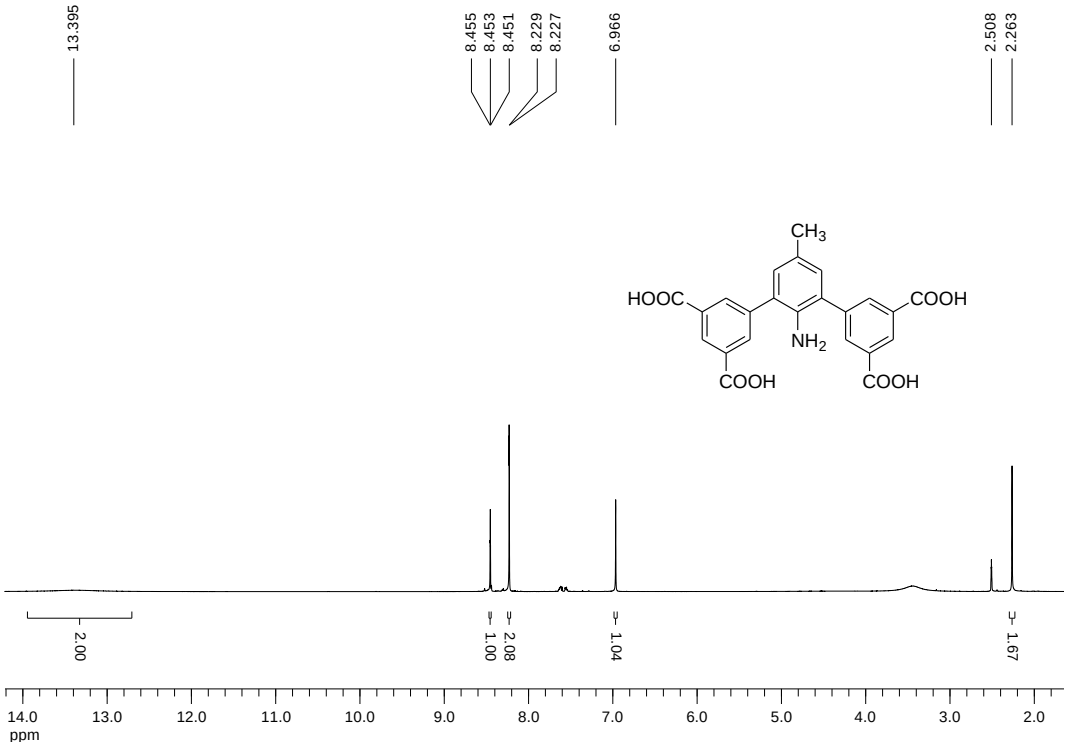
13.395
8.455
8.453
8.451
8.229
8.227
6.966
2.508
2.263
CH3
HOOC
COOH
NH2
COOH
COOH
2.00
1.00
2.08
1.04
1.67
14.0
13.0
12.0
11.0
10.0
9.0
8.0
7.0
6.0
5.0
4.0
3.0
2.0
ppm

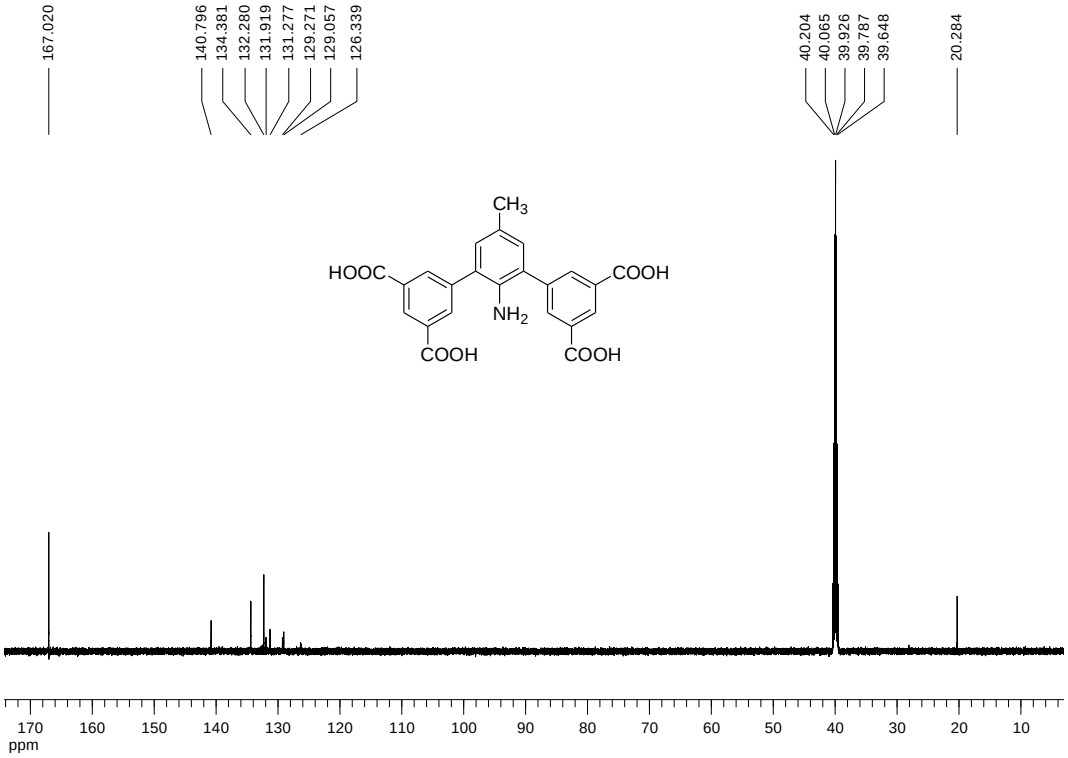
167.020
140.796
134.381
132.280
131.919
131.277
129.271
129.057
126.339
40.204
40.065
39.926
39.787
39.648
20.284
CH3
HOOC
COOH
NH2
COOH
COOH
170 160 150 140 130 120 110 100 90 80 70 60 50 40 30 20 10
ppm

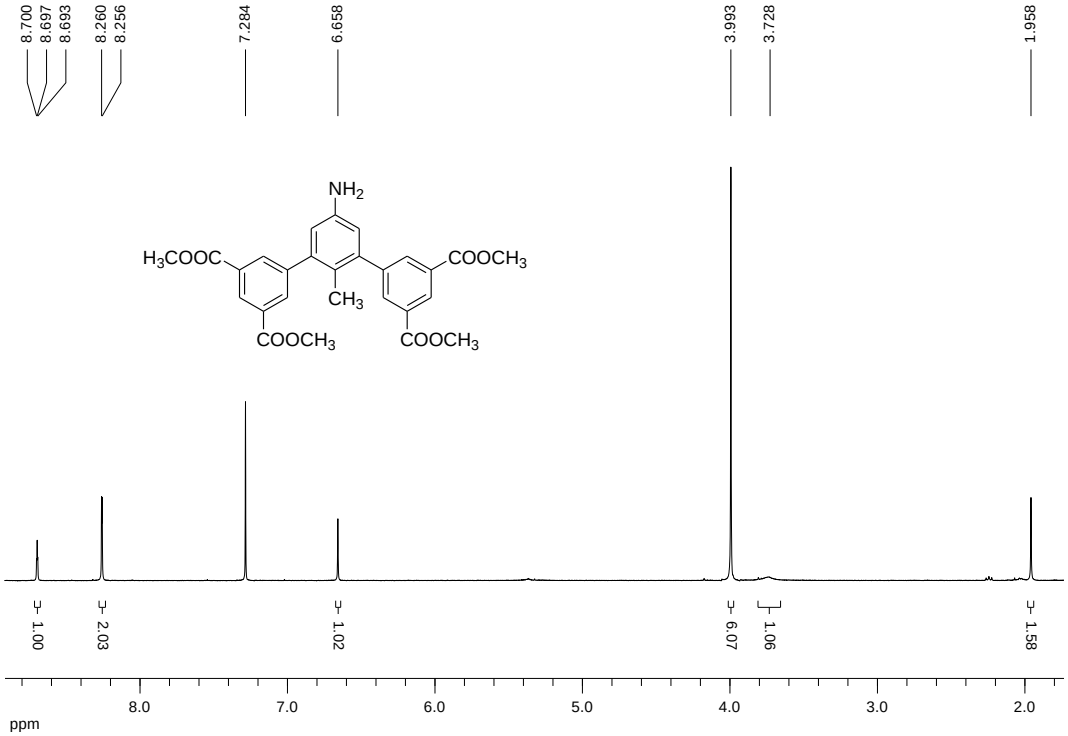
8.700
8.697
8.693
8.260
8.256
7.284
6.658
3.993
3.728
1.958
NH2
H3COOC
COOCH3
CH3
COOCH3
COOCH3
1.00
2.03
1.02
6.07
1.06
1.58
8.0 7.0 6.0 5.0 4.0 3.0 2.0
ppm

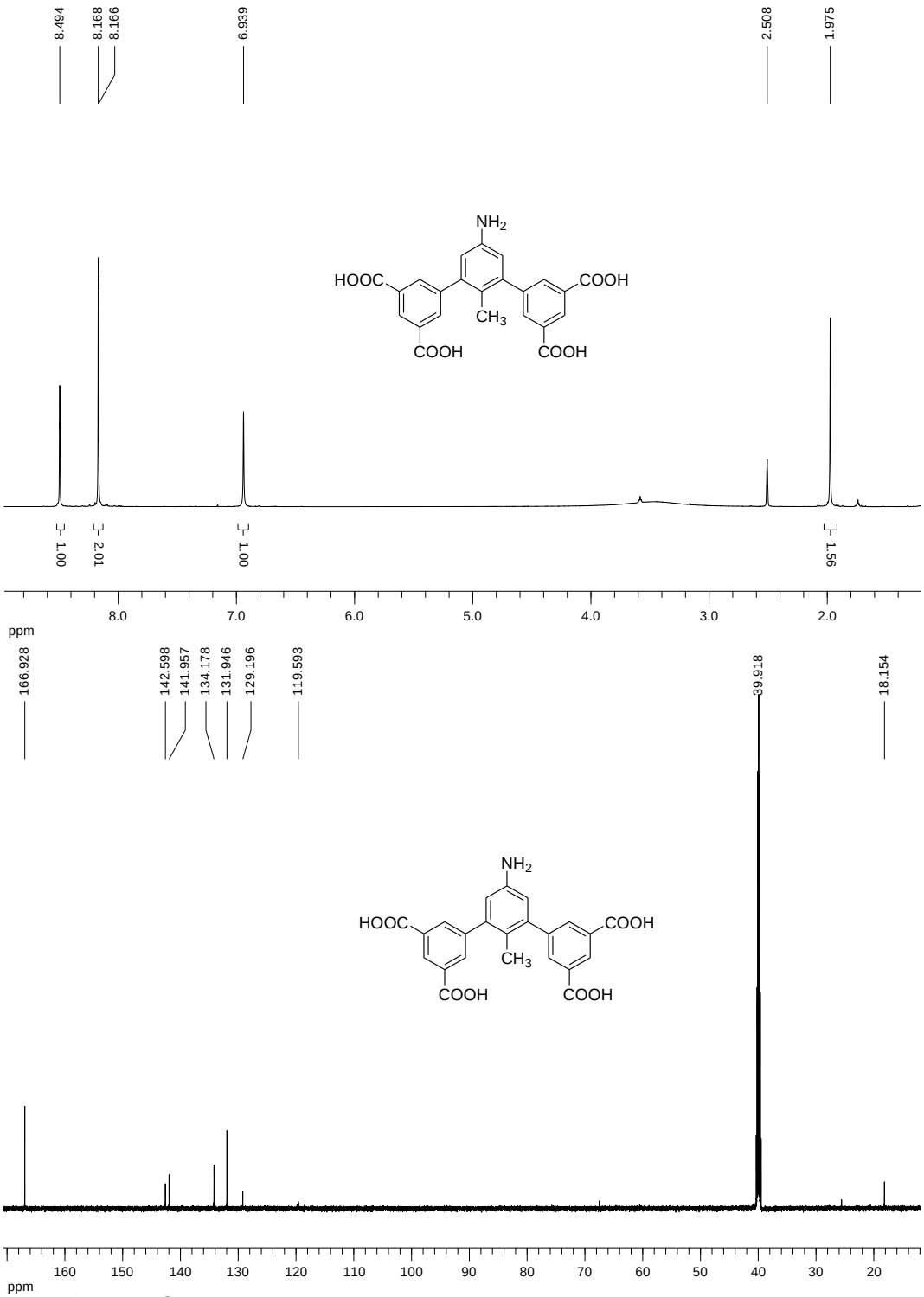

Fig. S8 ^{1}H and ^{13}C NMR spectra.

Table S1 Crystal data and structure refinement for **ZJNU-11** and **ZJNU-12**.

MOFs	**ZJNU-11**	**ZJNU-12**
Empirical formula	$C_{23}H_{17}Cu_2NO_{10}$	$C_{23}H_{17}Cu_2NO_{10}$
Formula weight	594.46	594.46
λ (Å)	1.54178	1.54178
Crystal system	Hexagonal	Hexagonal
Space group	$P6_3/mmc$	$P6_3/mmc$
Unit cell dimensions	a = 18.5626(7) Å b = 18.5626(7) Å c = 23.7453(10) Å α = 90° β = 90° γ = 120°	a = 18.6231(7) Å b = 18.6231(7) Å c = 23.8591(10) Å α = 90° β = 90° γ = 120°
V (Å^3)	7085.7(6)	7166.2(6)
Z	6	6
D_c (g cm^{-3})	0.836	0.826
μ (mm^{-1})	1.374	1.359
F(000)	1800	1800
θ range for data collection (°)	3.320 to 65.197	5.791 to 68.181
Limiting indices	$-21 \leq h \leq 17$ $-15 \leq k \leq 21$ $-25 \leq l \leq 27$	$-22 \leq h \leq 22$ $-22 \leq k \leq 22$ $-26 \leq l \leq 28$
Reflections collected / unique	24310 / 2272	53611 / 2464
R_{int}	0.0652	0.1458
Max. and min. transmission	0.876 and 0.820	0.873 and 0.822
Refinement method	Full-matrix least-squares on F^2	Full-matrix least-squares on F^2
Data/restraints/parameters	2272 / 0 / 107	2464 / 19 / 107
Goodness-of-fit on F^2	1.091	1.034
Final R indices [$I > 2\sigma(I)$]	R_1 = 0.0677 wR_2 = 0.2631	R_1 = 0.0488 wR_2 = 0.1705
R indices (all data)	R_1 = 0.0776 wR_2 = 0.2745	R_1 = 0.0717 wR_2 = 0.2016
Largest diff. peak and hole (e·Å^{-3})	0.241 and -0.369	1.131 and -0.579
CCDC	1921552	1921553

Table S2 Langmuir-Freundlich parameters for adsorption of C_2H_2, CO_2, and CH_4 in **ZJNU-11**.

Adsorbed component	q_{sat} (mmol g^{-1})	b_0 $(kPa)^{-v}$	E (kJ mol^{-1})	v	R^2
C_2H_2	13.17848	6.84322×10^{-6}	21.760	0.78229	0.99978
CO_2	15.82271	2.22604×10^{-7}	24.218	1	0.99997
CH_4	10.1892	1.13099×10^{-6}	17.063	1	0.99992

Table S3 Summary of gas adsorption properties of **ZJNU-11** and **ZJNU-12**.

MOFs	S_{BET} ($m^2 g^{-1}$)	$S_{Langmuir}$ ($m^2 g^{-1}$)	V_p ($cm^3 g^{-1}$)	D_c ($g\ cm^{-3}$)	C_2H_2 uptake[a] ($cm^3 g^{-1}$, STP)			CO_2 uptake[a] ($cm^3 g^{-1}$, STP)			CH_4 uptake[a] ($cm^3 g^{-1}$, STP)			C_2H_2/CH_4 (50/50, *v*/*v*) IAST selectivity[a]			CO_2/CH_4 (50/50, *v*/*v*) IAST selectivity[a]		
					298 K	288 K	278 K	298 K	288 K	278 K	298 K	288 K	278 K	298 K	288 K	278 K	298 K	288 K	278 K
ZJNU-11	1860	2166	0.7734	0.7851	186.2	206.9	227.8	105.0	131.1	162.0	24.0	30.0	37.1	36.2	41.6	49.1	5.9	6.6	7.6
ZJNU-12	1208	1404	0.5028	0.7763	122.9	134.0	144.4	74.6	91.6	112.2	17.8	22.1	27.2	35.4	41.9	50.9	5.9	6.7	7.8

$S_{BET}/S_{Langmuir}$ = BET and Langmuir surface areas; V_p = Pore volume based on 77 K N_2 isotherm; D_c = Framework density calculated from single-crystal X-ray data; [a] at 1 atm.

Table S4 Summaries of C_2H_2 and CO_2 adsorption properties of some reported dicopper paddlewheel-based MOFs constructed from linear/bent diisophthalate ligands.

MOFs	Ligand structure	S_{BET} (m^2 g^{-1})	V_p (cm^3 g^{-1})	C_2H_2 uptake (cm^3 g^{-1}, STP)	CO_2 uptake (cm^3 g^{-1}, STP)	*Ref.*
NJU-Bai17	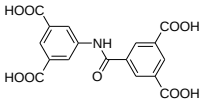	2423	0.914	222.4 (296 K/1 bar)	NA	1
ZJU-195	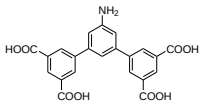	1786.9	0.93	214.2 (298 K/1 atm)	105.0 (298 K/1 atm)	2
UTSA-90	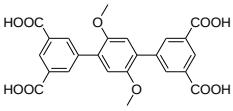	2273	0.88	214.0 (295 K/1 bar)	125 (295 K/1 bar)	3
ZJNU-47	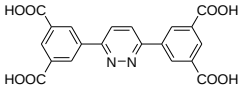	2638	1.031	213 (295 K/1 atm)	NA	4
ZJNU-84	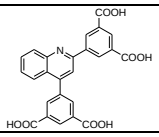	1926	0.7758	210.3 (298 K/1 atm)	122.6 (298 K/1 atm)	5
ZJNU-57	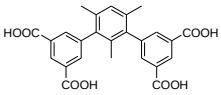	1935	0.768	201.5 (298 K/1 atm)	112.2 (298 K/1 atm)	6
ZJNU-71	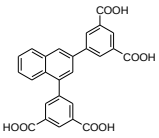	1860	0.7523	200.4 (298 K/1 atm)	115.6 (298 K/1 atm)	7
ZJNU-59	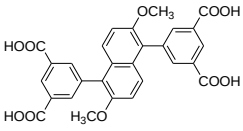	2043	0.781	199.5 (298 K/1 atm)	109.4 (298 K/1 atm)	8
ZJNU-98	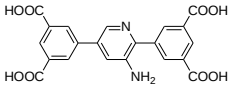	2378	0.9324	194.3 (298 K/1 atm)	99.2 (298 K/1 atm)	9
ZJNU-34	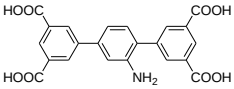	2459	0.9687	193.8 (298 K/1 atm)	96.2 (298 K/1 atm)	10
ZJU-5	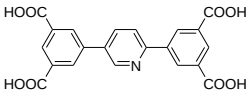	2823	1.074	193 (298 K/1 bar)	NA	11

ZJNU-48	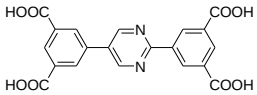	2670	1.044	193 (295 K/1 atm)	NA	4
ZJNU-99	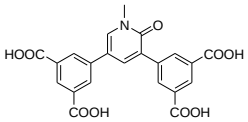	2113	0.835	189.8 (298 K/1 atm)	102.5 (298 K/1 atm)	12
ZJNU-56	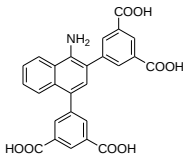	1655	0.653	189 (298 K/1 atm)	122 (298 K/1 atm)	13
ZJNU-46	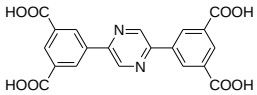	2622	1.025	187 (295 K/1 atm)	NA	4
ZJNU-11	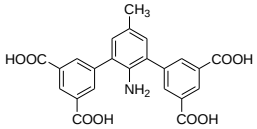	1860	0.7734	186.2 (298 K/1 atm)	105.0 (298 K/1 atm)	This work
ZJNU-96	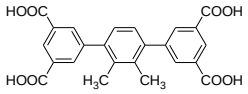	2352	0.934	183.6 (298 K/1 atm)	88.7 (298 K/1 atm)	14
ZJNU-89	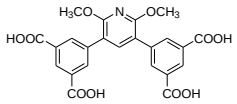	1618	0.63	181.3 (298 K/1 atm)	103.0 (298 K/1 atm)	15
ZJNU-74	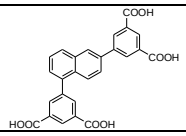	2243	0.8878	180.0 (298 K/1 atm)	88.1 (298 K/1 atm)	16
ZJU-10	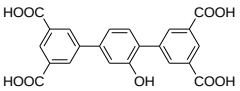	2392	0.9666	174 (298 K/1 atm)	81 (298 K/1 atm)	17
ZJNU-91	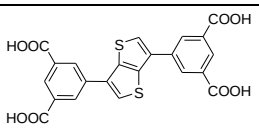	2404	0.982	172.5 (298 K/1 atm)	94.8 (298 K/1 atm)	18
ZJNU-88	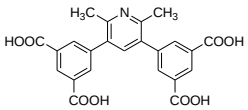	1693	0.70	166.0 (298 K/1 atm)	99.2 (298 K/1 atm)	15
Cu-DDC	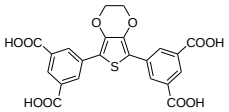	2410	0.98	164 (298 K/1 bar)	91 (298 K/1 bar)	19
ZJNU-93	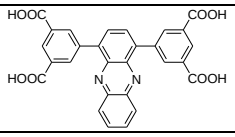	1952	0.7633	164.0 (298 K/1 atm)	96.2 (298 K/1 atm)	20
Cu_2(EBTC)	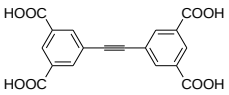	1852	1.01	160 (295 K/1 bar)	NA	21

ZJNU-58	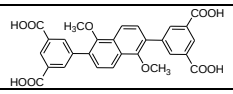	2487	0.976	157.1	81.6	8
ZJNU-92	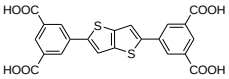	2845	1.103	155.1 (298 K/1 atm)	79.2 (298 K/1 atm)	18
UPC-21	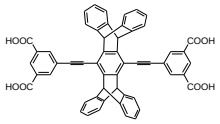	1725.1	0.69	139.5 (295 K/1 bar)	NA	22
UTSA-40	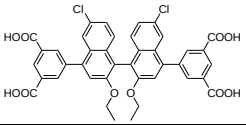	1630	0.65	124.6 (296 K/1 atm)	73.6 (296 K/1 atm)	23
ZJNU-78	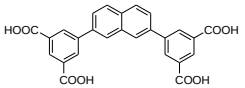	1311	0.521	122.0 (298 K/1 atm)	82.0 (298 K/1 atm)	24
ZJU-15	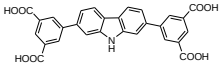	1660	0.67	100 (298 K/1 atm)	39 (298 K/1 atm)	25
ZJNU-51	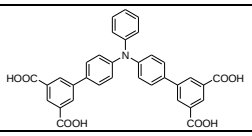	1382	0.5446	97.6 (298 K/1 atm)	59.3 (298 K/1 atm)	26
MFM-130	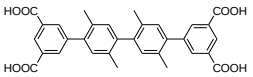	2173	1.0	85.9 (298 K/1 bar)	59 (298 K/1 bar)	27
ZJNU-44	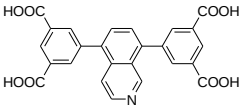	2314	0.9158	NA	116 (298 K/1 atm)	28
Cu_2L	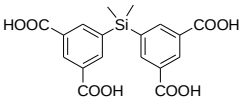	1145.9	0.998	NA	115 (298 K/1 bar)	29
Cu_2cdip	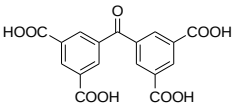	1539	0.81	NA	111.3 (298 K/1 bar)	30
ZJNU-40	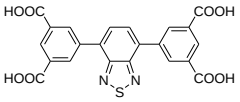	2209	0.88	NA	108 (296 K/1 atm)	31
ZJNU-45	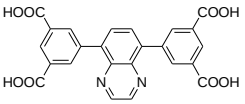	2232	0.8774	NA	107 (298 K/1 atm)	28
Cu_2L	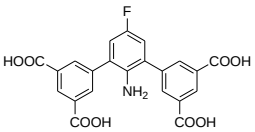	1580	0.97	NA	106 (298 K/1 bar)	32
Cu_2L	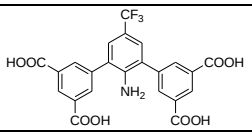	1584	0.6	NA	106 (298 K/1 bar)	33

Cu_2L	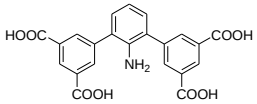	1410	0.97	NA	104.39 (298 K/1 bar)	34
ZJNU-43	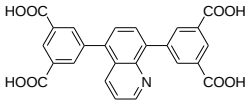	2243	0.8943	NA	103 (298 K/1 atm)	28
QI-Cu	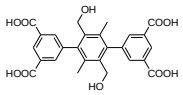	1631	0.662	NA	102.2 (293 K/1 bar)	35
GDMU-2	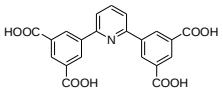	1860	0.80	NA	102 (273 K/1 bar)	36
NJU-Bai14	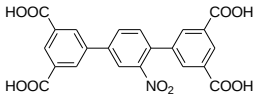	2383	0.92	NA	100 (298 K/1 bar)	37
NJFU-3	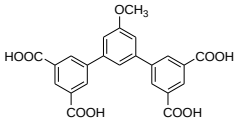	2531.1	0.94	NA	95.6 (298 K/1 bar)	38
PCN-88	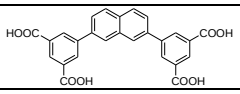	3308	NA	NA	94 (296 K/1 atm)	39
HNUST-1	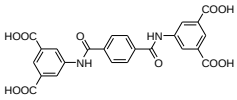	1400	0.571	NA	93.0 (298 K/1 bar)	40
HNUST-3	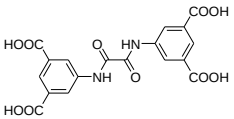	2412	0.99	NA	84.5 (298 K/1 atm)	41
JUC-1000	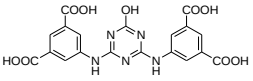	1221	0.48	NA	80 (298 K/1 atm)	42
SNU-50	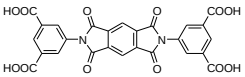	2300	1.08	NA	80 (298 K/1 bar)	43
PCN-308	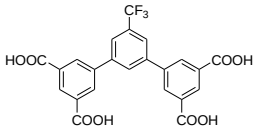	1418	0.810	NA	78.4 (298 K/1 bar)	44
PCN-305	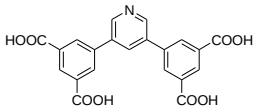	1720	0.926	NA	73.8 (298 K/1 bar)	44
PCN-307	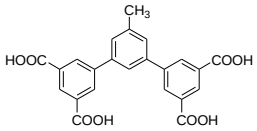	1376	0.808	NA	73.3 (298 K/1 bar)	44
PCN-306	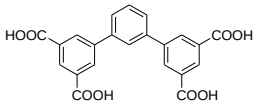	1927	1.043	NA	70.3 (298 K/1 bar)	44

HNUST-7	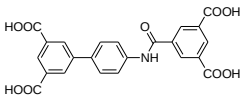	2804	1.11	NA	68.05 (298 K/1 atm)	45
HNUST-6	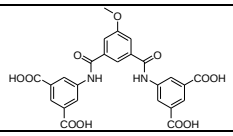	1093	0.455	NA	67.3 (298k/1bar)	46
HNUST-4	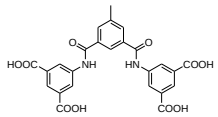	1136	0.458	NA	62.9 (298 K/1 atm)	47
UHM-6	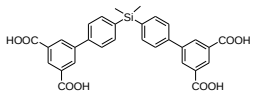	1164	0.46	NA	47 (298 K/1 bar)	48

S_{BET} = BET specific surface area; V_p = pore volume; NA = not available

Reference

1. Zhang, M.; Li, B.; Li, Y.; Wang, Q.; Zhang, W.; Chen, B.; Li, S.; Pan, Y.; You, X.; Bai, J., Finely Tuning MOFs towards High-performance in C_2H_2 Storage: Synthesis and Properties of a New MOF-505 Analogue with the Inserted Amide Functional Group. *Chem. Commun.* **2016,** *52*, 7241-7244.
2. Zhang, L.; Jiang, K.; Li, Y.; Zhao, D.; Yang, Y.; Cui, Y.; Chen, B.; Qian, G., Microporous Metal-Organic Framework with Exposed Amino Functional Group for High Acetylene Storage and Excellent C_2H_2/CO_2 and C_2H_2/CH_4 Separations. *Cryst. Growth Des.* **2017,** *17*, 2319-2322.
3. Wen, H.-M.; Chang, G.; Li, B.; Lin, R.-B.; Hu, T.-L.; Zhou, W.; Chen, B., Highly Enhanced Gas Uptake and Selectivity via Incorporating Methoxy Groups into a Microporous Metal-Organic Framework. *Cryst. Growth Des.* **2017,** *17*, 2172-2177.
4. Song, C.; Jiao, J.; Lin, Q.; Liu, H.; He, Y., C_2H_2 Adsorption in Three Isostructural Metal-Organic Frameworks: Boosting C_2H_2 Uptake by Rational Arrangement of Nitrogen Sites. *Dalton Trans.* **2016,** *45* (11), 4563-4569.
5. Bai, D.; Gao, X.; He, M.; Wang, Y.; He, Y., Three isoreticular MOFs derived from nitrogen-functionalized diisophthalate ligands: exploring the positional effect of nitrogen functional sites on the structural stabilities and selective C_2H_2/CH_4 and CO_2/CH_4 adsorption properties. *Inorg. Chem. Front.* **2018,** *5* (36), 1423-1431.
6. Wang, Y.; He, M.; Tian, Z.; Zhong, H.; Zhu, L.; Zhang, Y.; Zhang, X.; Chen, D.-L.; He, Y., Rational Construction of a ssa-Type of MOF through Preorganizing the Ligand's Conformation and Its Exceptional Gas Adsorption Properties. *Dalton Trans.* **2018,** *47* (7), 2444-2452.
7. Chen, F.; Bai, D.; Jiang, D.; Wang, Y.; He, Y., A Comparative Study of C_2H_2 Adsorption Properties in Five Isomeric Copper-Based MOFs Based on Naphthalene-Derived Diisophthalates. *Dalton Trans.* **2017,** *46* (34), 11469 -11478.
8. Wang, Y.; He, M.; Gao, X.; Li, S.; Xiong, S.-s.; Krishna, R.; He, Y., Exploring the Effect of Ligand-Originated MOF Isomerism and Methoxy Group Functionalization on Selective Acetylene/Methane and Carbon Dioxide/Methane Adsorption Properties in Two NbO-Type MOFs. *ACS Appl. Mater. Interfaces* **2018,** *10* (24), 20559-20568.
9. He, M.; Xu, T.; Jiang, Z.; Yang, L.; Zou, Y.; Xia, F.; Wang, X.; Wang, X.; He, Y., Incorporation of bifunctional aminopyridine into a NbO-type MOF for markedly enhanced adsorption of CO_2 and C_2H_2 over CH_4. *Inorg. Chem. Front.* **2019,** *6* (5), 1177-1183.
10. Chen, F.; Bai, D.; Wang, X.; He, Y., A Comparative Study of the Effect of Functional Groups on C_2H_2 Adsorption in NbO-Type Metal-Organic Frameworks. *Inorg. Chem. Front.* **2017,** *4* (6), 960-967.
11. Rao, X.; Cai, J.; Yu, J.; He, Y.; Wu, C.; Zhou, W.; Yildirim, T.; Chen, B.; Qian, G., A Microporous Metal-Organic Framework with Both Open Metal and Lewis Basic Pyridyl Sites for High C_2H_2 and CH_4 Storage at Room Temperature. *Chem. Commun.* **2013,** *49* (60), 6719-6721.
12. He, M.; Xia, F.; Xu, T.; Gao, X.; Jiang, Z.; Wang, X.; He, Y., A lactam-functionalized copper-bent diisophthalate framework displaying significantly enhanced adsorption of CO_2 and C_2H_2 over CH_4. *Dalton Trans.* **2019**, 10.1039/C9DT01778J.
13. Jiao, J.; Jiang, D.; Chen, F.; Bai, D.; He, Y., A Porous Metal-Organic Framework Based on an Asymmetric Angular Diisophthalate for Selective Adsorption of C_2H_2 and CO_2 over CH_4. *Dalton Trans.* **2017,** *46* (24), 7813-7820.
14. He, M.; Jiang, T. X. Z.; Yu, X.; Zou, Y.; Yang, L.; Wang, X.; Wang, X.; He, Y., Two copper-based

MOFs constructed from a linear diisophthalate linker: supramolecular isomerism and gas adsorption properties. *CrystEngComm* **2019,** *21* (20), 3192-3198.

15. Wang, Y.; He, M.; Gao, X.; Long, P.; Zhang, Y.; Zhong, H.; Wang, X.; He, Y., Three Isoreticular ssa-type MOFs Derived from Bent Diisophthalate Ligands: Exploring the Substituent Effect on Structural Stabilities and Selective C_2H_2/CH_4 and CO_2/CH_4 adsorption properties. *Dalton Trans.* **2018,** *47* (36), 12702-12710.
16. Chen, F.; Bai, D.; Wang, Y.; Jiang, D.; He, Y., A Family of *ssa*-Type Copper-Based MOFs Constructed from Unsymmetrical Diisophthalates: Synthesis, Characterization and Selective Gas Adsorption. *Mater. Chem. Front.* **2017,** *1* (11), 2283-2291.
17. Duan, X.; Wang, H.; Ji, Z.; Cui, Y.; Yang, Y.; Qian, G., A novel metal-organic framework for high storage and separation of acetylene at room temperature. *J. Solid State Chem.* **2016,** *241*, 152-156.
18. Wang, Y.; He, M.; Gao, X.; Zhang, Y.; Zhong, H.; Long, P.; Wang, X.; He, Y., Two NbO-Type MOFs Based on Linear and Zigzag Diisophthalate Ligands: Exploring the Effect of Ligand-Originated MOF Isomerization on Gas Adsorption Properties. *Inorg. Chem. Front.* **2018,** *5* (11), 2811-2817.
19. Wang, F.; Kusaka, S.; Hijikata, Y.; Hosono, N.; Kitagawa, S., Development of a Porous Coordination Polymer with a High Gas Capacity Using a Thiophene-Based Bent Tetracarboxylate Ligand. *ACS Appl. Mater. Interfaces* **2017,** *9*, 33455-33460.
20. Li, S.; Wu, J.; Gao, X.; He, M.; Wang, Y.; Wang, X.; He, Y., A NbO-type MOF based on an aromatic-rich and N-functionalized diisophthalate ligand for high-performance acetylene storage and purification. *CrystEngComm* **2018,** *20* (44), 7178-7183.
21. Hu, Y.; Xiang, S.; Zhang, W.; Zhang, Z.; Wang, L.; Bai, J.; Chen, B., A new MOF-505 analog exhibiting high acetylene storage. *Chem. Commun.* **2009**, 7551-7553.
22. Zhang, M.; Xin, X.; Xiao, Z.; Wang, R.; Zhang, L.; Sun, D., A multi-aromatic hydrocarbon unit induced hydrophobic metal–organic framework for efficient C_2/C_1 hydrocarbon and oil/water separation. *J. Mater. Chem. A* **2017,** *5*, 1168-1175
23. He, Y.; Xiang, S.; Zhang, Z.; Xiong, S.; Wu, C.; Zhou, W.; Yildirim, T.; Krishna, R.; Chen, B., A microporous metal-organic framework assembled from an aromatic tetracarboxylate for H_2 purification. *J. Mater. Chem. A* **2013,** *1* (7), 2543-2551.
24. Chen, F.; Bai, D.; Wang, Y.; He, M.; Gao, X.; He, Y., A Pair of Polymorphous Metal-Organic Frameworks Based on an Angular Diisophthalate Linker: Synthesis, Characterization and Gas Adsorption Properties. *Dalton Trans.* **2018,** *47* (3), 716-725.
25. Duan, X.; Zhou, Y.; Lv, R.; Yu, B.; Chen, H.; Jia, Z.; Cui, Y.; Yang, Y.; Qian, G., A new metal-organic framework for separation of C_2H_2/CH_4 and CO_2/CH_4 at room temperature. *J. Solid State Chem.* **2018,** *260*, 31-33.
26. Wang, Y.; He, M.; Gao, X.; Li, S.; He, Y., A Metal-Organic Framework Based on a Custom-Designed Diisophthalate Ligand Exhibiting Excellent Hydrostability and Highly Selective Adsorption of C_2H_2 and CO_2 over CH_4. *Dalton Trans.* **2018,** *47* (21), 7213 -7221.
27. Yan, Y.; Juríček, M.; Coudert, F.-X.; Vermeulen, N. A.; Grunder, S.; Dailly, A.; Lewis, W.; Blake, A. J.; Stoddart, J. F.; Schröder, M., Non-Interpenetrated Metal-Organic Frameworks Based on Copper(II) Paddlewheel and Oligoparaxylene-Isophthalate Linkers: Synthesis, Structure, and Gas Adsorption. *J. Am. Chem. Soc.* **2016,** *138*, 3371-3381.
28. Song, C.; Hu, J.; Ling, Y.; Feng, Y.; Krishna, R.; Chen, D.-l.; He, Y., The Accessibility of Nitrogen Sites Makes Difference to Selective CO_2 Adsorption in a Family of Isostructural Metal-Organic

Frameworks. *J. Mater. Chem. A* **2015,** *3* (38), 19417-19426.

29. Gao, C.-Y.; Tian, H.-R.; Ai, J.; Li, L.-J.; Dang, S.; Lan, Y.-Q.; Sun, Z.-M., A microporous Cu-MOF with optimized open metal sites and pore spaces for high gas storage and active chemical fixation of CO_2. *Chem. Commun.* **2016,** *52*, 11147-11150.
30. Feng, G.; Peng, Y.; Liu, W.; Chang, F.; Dai, Y.; Huang, W., Polar Ketone-Functionalized Metal-Organic Framework Showing a High CO_2 Adsorption Performance. *Inorg. Chem.* **2017,** *56*, 2363-2366.
31. Song, C.; He, Y.; Li, B.; Ling, Y.; Wang, H.; Feng, Y.; Krishna, R.; Chen, B., Enhanced CO_2 sorption and selectivity by functionalization of a NbO-type metal-organic framework with polarized benzothiadiazole moieties. *Chem. Commun.* **2014,** *50* (81), 12105-12108.
32. Pal, T. K.; De, D.; Senthilkumar, S.; Neogi, S.; Bharadwaj, P. K., A Partially Fluorinated, Water-Stable Cu(II)-MOF Derived via Transmetalation: Significant Gas Adsorption with High CO_2 Selectivity and Catalysis of Biginelli Reactions. *Inorg. Chem.* **2016,** *55*, 7835-7842.
33. Gupta, A. K.; De, D.; Tomar, K.; Bharadwaj, P. K., A Cu(II) metal-organic framework with significant H2 and CO2 storage capacity and heterogeneous catalysis for the aerobic oxidative amination of C(sp^3)-H bond and Biginelli reactions. *Dalton Trans.* **2017,** *47*, 1624-1634
34. Pal, T. K.; De, D.; Neogi, S.; Pachfule, P.; Senthilkumar, S.; Xu, Q.; Bharadwaj, P. K., Significant Gas Adsorption and Catalytic Performance by a Robust CuII–MOF Derived through Single-Crystal to Single-Crystal Transmetalation of a Thermally Less-Stable ZnII–MOF. *Chem. Eur. J.* **2015,** *21*, 19064-19070.
35. Wang, C.; Li, L.; Tang, S.-F.; Zhao, X., Enhanced uptake and selectivity of CO_2 adsorption in a hydrostable metal-organic frameworks via incorporating methylol and methyl groups. *ACS Appl. Mater. Interfaces* **2014,** *6*, 16932-16940.
36. Liu, J.; Wang, W.; Luo, Z.; Li, B.; Yuan, D., Microporous Metal-Organic Framework Based on Ligand-Truncation Strategy with High Performance for Gas Adsorption and Separation. *Inorg. Chem.* **2017,** *56*, 10215-10219.
37. Zhang, M.; Wang, Q.; Lu, Z.; Liu, H.; Liu, W.; Bai, J., A nitro-decorated NbO-type metal-organic framework with highly selective CO_2 uptake and CH_4 storage capacity. *CrystEngComm* **2014,** *16*, 6287-6290.
38. Du, L.; Lu, Z.; Xu, L.; Zhang, J., A new mfj-type metal-organic framework constructed from a methoxyl derived V-shaped ligand and its H_2, CO_2 and CH_4 adsorption properties. *RSC Adv.* **2017,** *7*, 21268-21272.
39. Li, J.-R.; Yu, J.; Lu, W.; Sun, L.-B.; Sculley, J.; Balbuena, P. B.; Zhou, H.-C., Porous materials with pre-designed single-molecule traps for CO_2 selective adsorption. *Nature Commun.* **2013,** *4*, 1538.
40. Zheng, B.; Liu, H.; Wang, Z.; Yu, X.; Yia, P.; Bai, J., Porous NbO-type metal-organic framework with inserted acylamide groups exhibiting highly selective CO_2 capture. *CrystEngComm* **2013,** *15*, 3517-3520.
41. Wang, Z.; Zheng, B.; Liu, H.; Lin, X.; Yu, X.; Yi, P.; Yun, R., High-Capacity Gas Storage by a Microporous Oxalamide-Functionalized NbO-Type Metal-Organic Framework. *Cryst. Growth Des.* **2013,** *13*, 5001-5006.
42. He, H.; Sun, Q.; Gao, W.; Perman, J. A.; Sun, F.; Zhu, G.; Aguila, B.; Forrest, K.; Space, B.; Ma, S., A Stable Metal-Organic Framework Featuring Local Buffer Environment for Carbon Dioxide Fixation. *Angew. Chem. Int. Ed.* **2018,** *57*, 4657-4662.

43. Prasad, T. K.; Hong, D. H.; Suh, M. P., High Gas Sorption and Metal-Ion Exchange of Microporous Metal-Organic Frameworks with Incorporated Imide Groups. *Chem. Eur. J.* **2010,** *16*, 14043-14050.
44. Liu, Y.; Li, J.-R.; Verdegaal, W. M.; Liu, T.-F.; Zhou, H.-C., Isostructural Metal-Organic Frameworks Assembled from Functionalized Diisophthalate Ligands through a Ligand-Truncation Strategy. *Chem. Eur. J.* **2013,** *19*, 5637-5643.
45. Zheng, B.; Huang, L.; Cao, X.; Shen, S.; Cao, H.; Hang, C.; Zeng, W.; Wang, Z., A highly porous acylamide decorated MOF-505 analogue exhibiting high and selective CO_2 gas uptake capability. *CrystEngComm* **2018,** *20*, 1874-1881
46. Wang, Z.; Luo, X.; Zheng, B.; Huang, L.; Hang, C.; Jiao, Y.; Cao, X.; Zeng, W.; Yun, R., Highly Selective Carbon Dioxide Capture and Cooperative Catalysis of a Water-Stable Acylamide-Functionalized Metal-Organic Framework. *Eur. J. Inorg. Chem.* **2018**, 1309-1314.
47. Zheng, B.; Lin, X.; Wang, Z.; Yun, R.; Fan, Y.; Ding, M.; Hua, X.; Yi, P., Enhanced water stability of a microporous acylamide-functionalized Metal-Organic Framework via interpenetration and methyl decoration. *CrystEngComm* **2014,** *16*, 9586-9589.
48. Frahm, D.; Fischer, M.; Hoffmann, F.; Fröba, M., An Interpenetrated Metal-Organic Framework and Its Gas Storage Behavior: Simulation and Experiment. *Inorg. Chem.* **2011,** *50*, 11055-11063.